SUPPLEMENTARY FIGURES

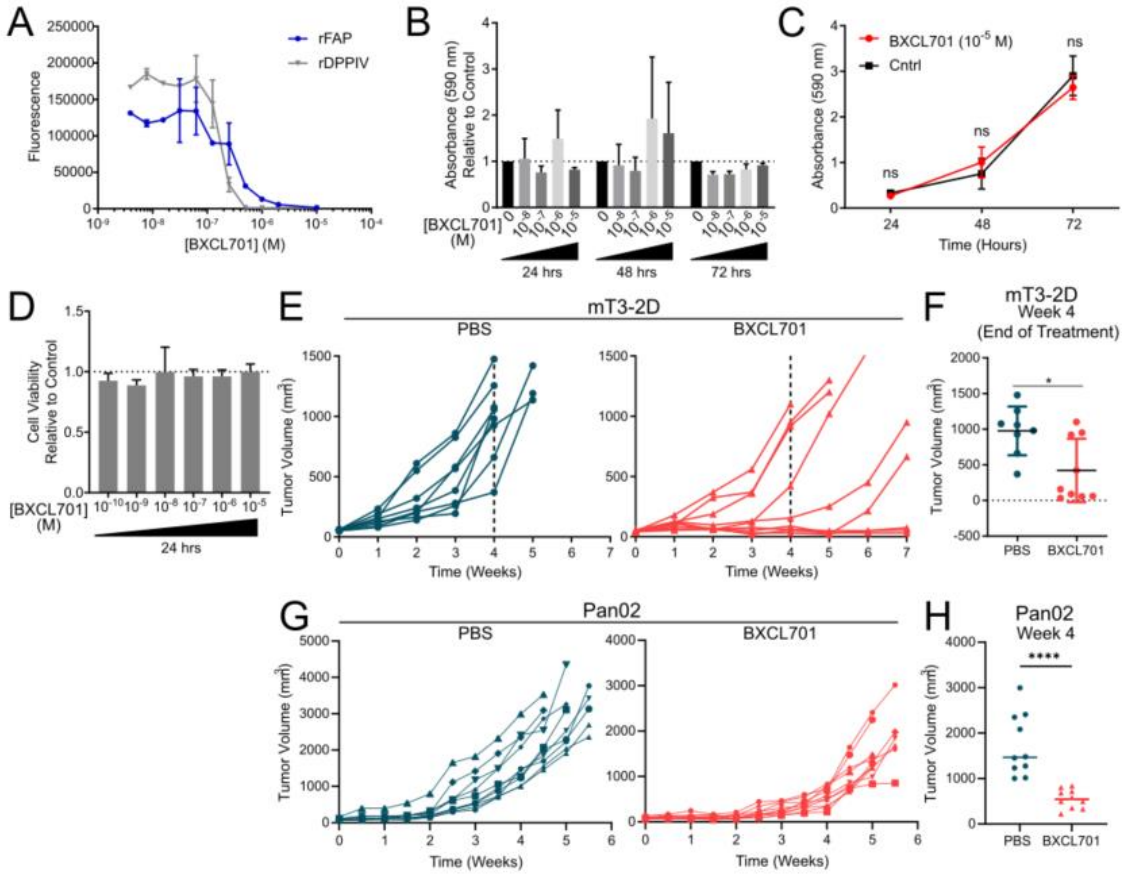

Supplementary Figure 1. DPP expression and inhibition in PDAC models. (A) Dipeptidyl peptidase activity assay confirming BXCL701 inhibits rFAP and rDPP4 activity *in vitro.*(B) Crystal violet cell proliferation assay demonstrating increasing concentrations of BXCL701 has no effect on mT3-2D cell proliferation *in vitro* at 24, 48 or 72 hours. (C) Crystal violet cell proliferation assay demonstrating 10^{-5} M BXCL701 has no effect on mT3-2D cell proliferation *in vitro*. Ns= nonsignificant as determined by unpaired two-tailed t-test. (D) Cell titer blue cytotoxicity assay demonstrating BXCL701 has no effect on cell viability *in vitro*. (E) Individual mT3-2D tumor growth curves for PBS and BXCL701 treated mice (n=10 per group). (F) Individual mT3-2D tumor volumes for PBS (n=8) and BXCL701(n=9) treated mice at week 4

(end of treatment). *p<0.05 by unpaired two-tailed t-test. (G) Individual Pan02 tumor growth curves for PBS and BXCL701 treated mice (n=10 per group). (H) Individual Pan02 tumor volumes for PBS (n=10) and BXCL701(n=10) treated mice after 4 weeks of treatment. ****p<0.0001 by unpaired two-tailed t-test.

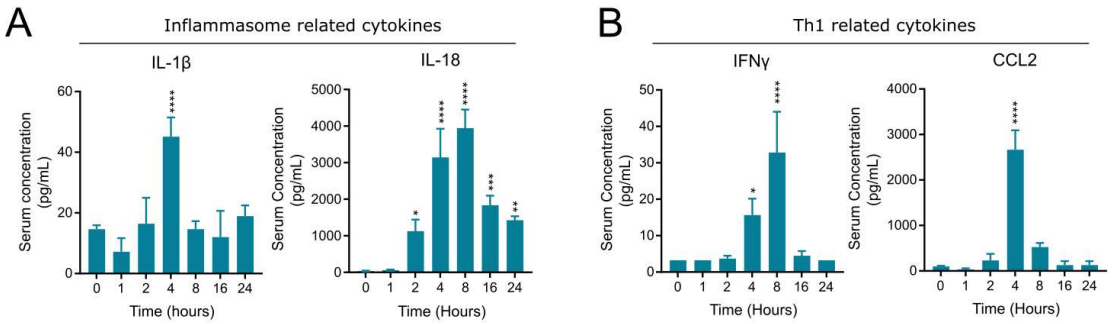

Supplemental Figure 2. BXCL701 increases circulating inflammasome and Th1-related cytokines in Balb/c mice bearing Wehi164 fibrosarcoma tumors. (A) Serum concentrations of inflammasome related cytokines in tumor bearing mice after exposure to 20 ug of BXCL701 at timepoint 0. *p<0.05, **p<0.01, ***p<0.001, ****p<0.0001 calculated by ANOVA then Dunnett's multiple comparison test. (B) Serum concentrations of Th1 related cytokines in tumor bearing mice after exposure to 20 ug of BXCL701 at timepoint 0. *p<0.05, ****p<0.0001 calculated by ANOVA then Dunnett's multiple comparison test.

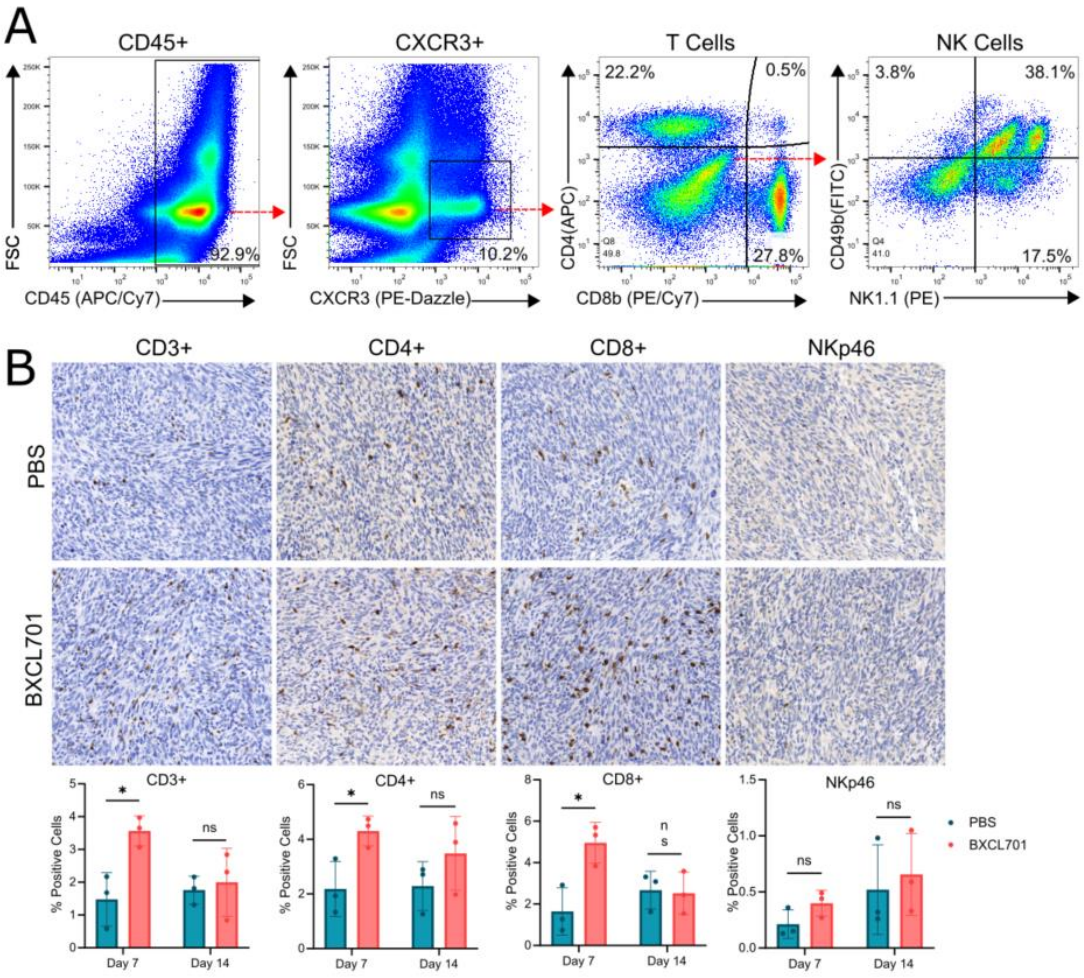

Supplementary Figure 3. Effect of BXCL701 on PDAC cell growth and tumoral immune cell content. (A) Representative flow cytometry gating for CD4+ T, CD8+T and NK1.1/CD49b+ murine splenocytes that express CXCR3. (B) Representative IHC images (taken at Day 7) and quantification of CD3, CD4, CD8 and NKp46 staining in PBS and BXCL701 treated Pan02 tumors (3 tumors/group). *p<0.05 as determined by unpaired two-tailed t-test

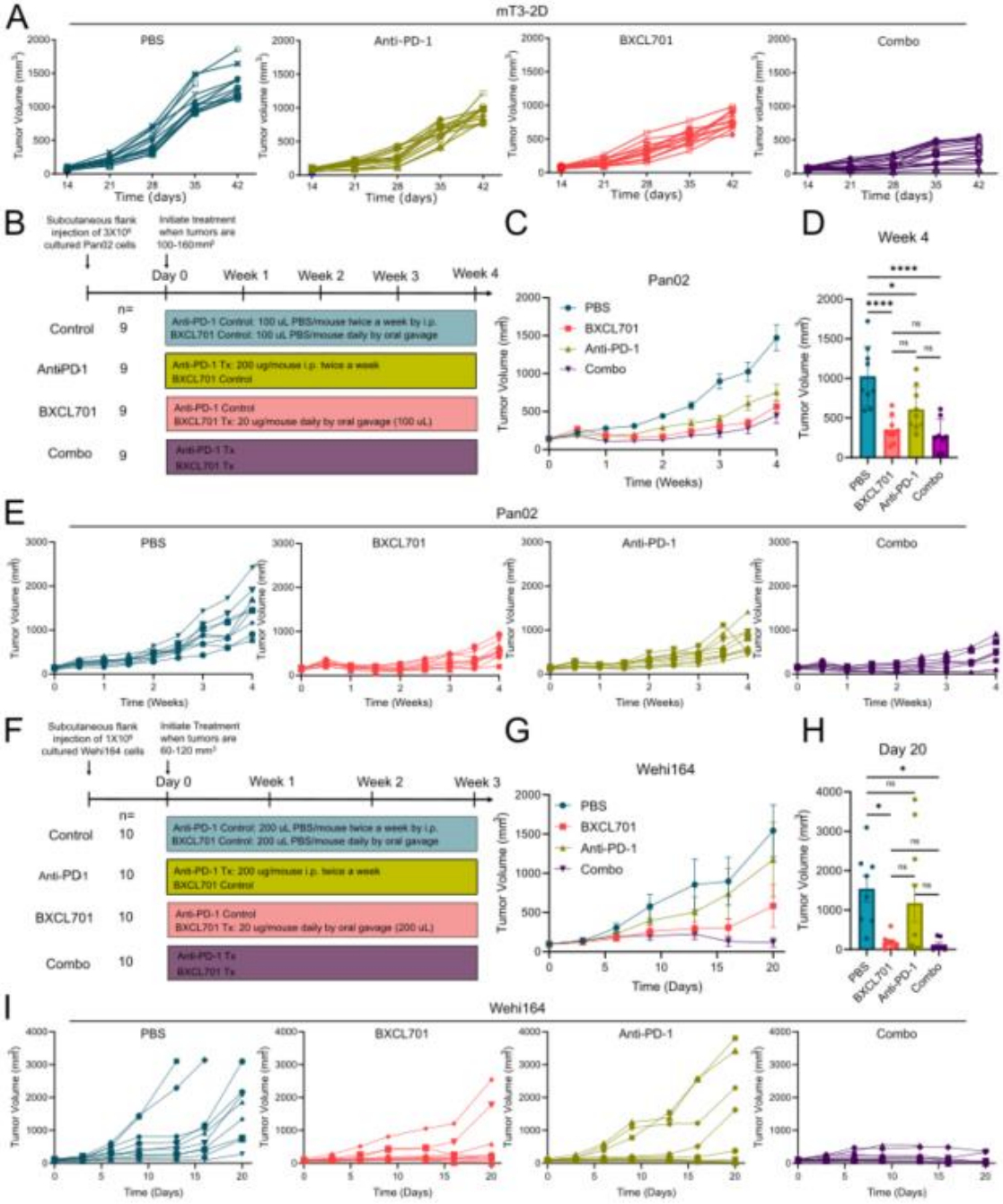

Supplemental Figure 4. BXCL701+anti-PD-1 treatment in additional murine models. (A) Individual growth curves for PBS control, anti-PD-1, BXCL701 or anti-PD-1 and BXCL701 ("combo") treated mice bearing mT3-2D tumors (n=15 per group). (B) Schematic of *in vivo*

experimental design testing combination treatment of BXCL701 and anti-PD-1 versus single agents alone and PBS controls in Pan02 C57BL/6 PDAC model. (C) Average Pan02 tumor growth curves in C57BL/6 mice (n = 9 per group) treated with PBS, anti-PD-1, BXCL701 and anti-PD-1 with BXCL701 ("combo"). Tumor growth was monitored weekly. (D) Tumor volumes for PBS, anti-PD-1, BXCL701 or anti-PD-1 and BXCL701 treated Pan02 tumors at the end of treatment (week 4). (ns= nonsignificant, *p<0.05, ****p<0.0001 as determined by ANOVA followed by Tukey's multiple comparison's test). (E) Individual Pan02 tumor growth curves for PBS control, anti-PD-1, BXCL701 or anti-PD-1 and BXCL701 ("combo") treated mice (n=9 per group). (F) Schematic of *in vivo* experimental design testing combination treatment of BXCL701 and anti-PD-1 versus single agents alone and PBS controls in Wehi164 Balb/c fibrosarcoma model. (G) Average Wehi164 tumor growth curves in C57BL/6 mice (n = 10 per group) treated with PBS, anti-PD-1, BXCL701 and anti-PD-1 with BXCL701 ("combo"). Tumor growth was monitored weekly. (H) Tumor volumes for PBS, anti-PD-1, BXCL701 or anti-PD-1 and BXCL701 treated Wehi164 tumors at the end of treatment (day 20). Two values were removed from the BXCL701 treated group before analysis after they were identified as a statistical outliers via Rout's method. (ns= nonsignificant, *p<0.05 as determined by ANOVA followed by Tukey's multiple comparison's test). (I) Individual Wehi164 tumor growth curves for PBS control, anti-PD-1, BXCL701 or anti-PD-1 and BXCL701 ("combo") treated mice (n=10 per group).

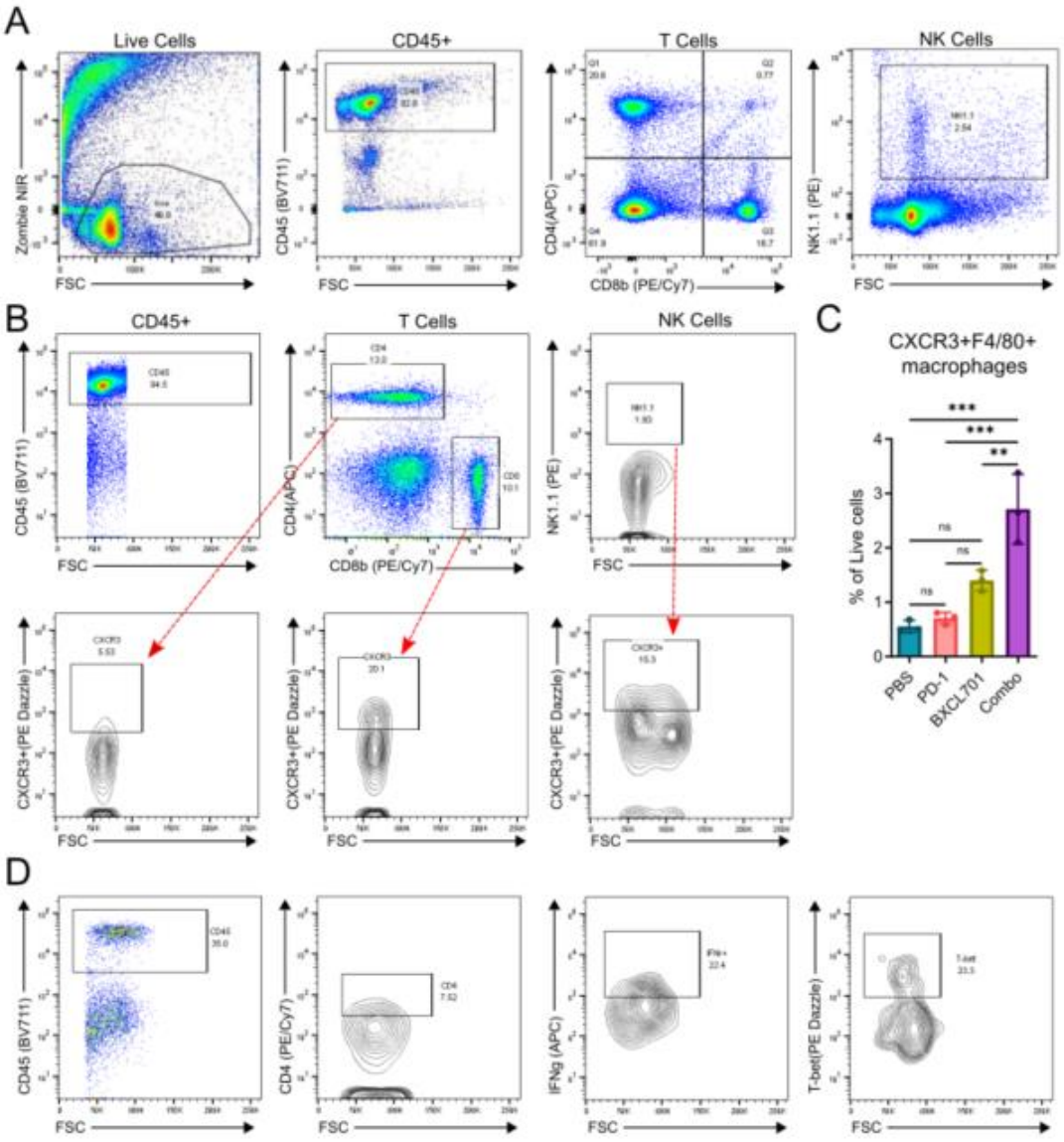

Supplemental Figure 5. Flow cytometry analysis of immune cell subtypes in BXCL701+anti-PC1 combination treated tumors. (A) Representative gating strategy for staining tumor infiltrating CD4+ T cells, CD8+ T cells and NK1.1+ NK cells. (B) Representative gating strategy for staining tumor infiltrating CXCR3+ CD4+ T cells, CXCR3+ CD8+ T cells and CXCR3+ NK1.1+ NK cells. (C) Flow cytometry data representing percentage of live cells that are CXCR3+F4/80+

macrophages in tumors from PBS, anti-PD-1, BXCL701 and combo treated mice (n = 3 per group, each dot representing 3-4 tumors from individual mice, **p<0.01, ***p<0.001, ns= nonsignificant as determined by one-way ANOVA followed by Tukey's multiple comparison test). (D) Representative gating strategy for staining tumor infiltrating CD4+IFNγ+Tbet+ Th1 cells.

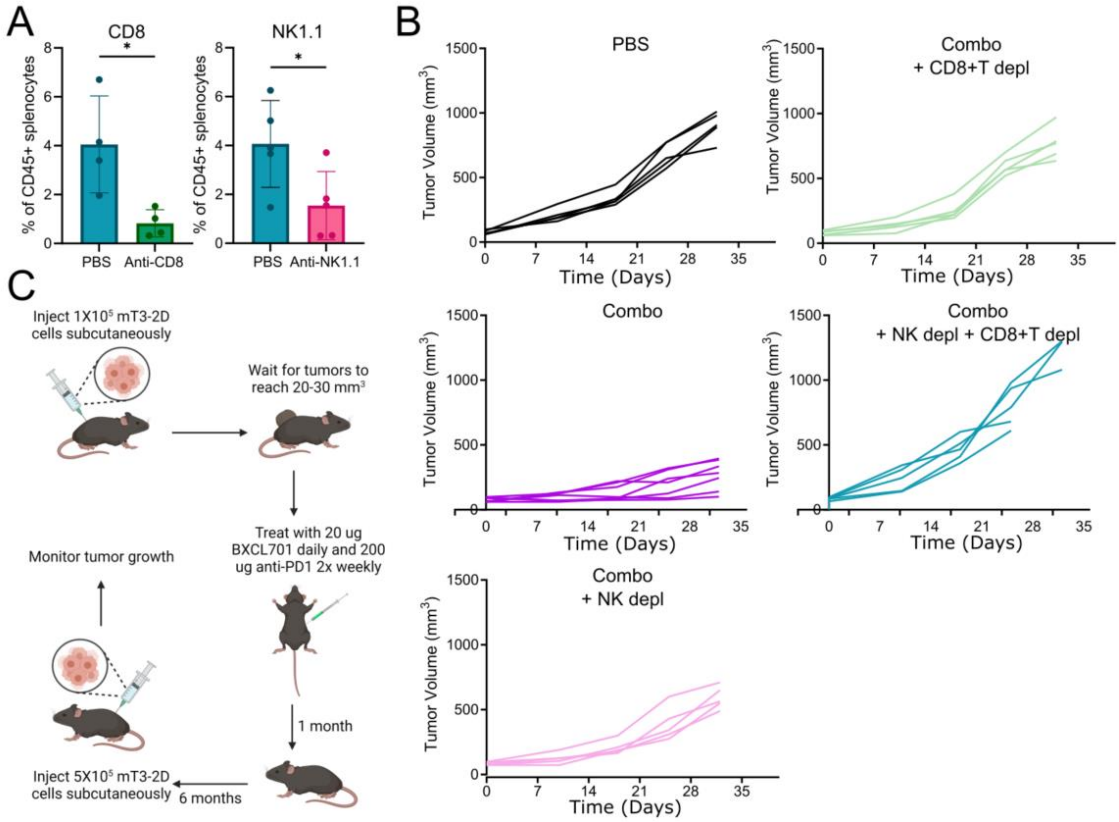

Supplementary Figure 6. BXCL701+anti-PD-1 combination treatment is dependent on CD8+T and NK cells. (A) Flow cytometry of splenocytes confirming successful depletion of CD8+ T cells and/or NK1.1+ cells. (CD8 T n=4 per treatment group; NK1.1 n=5 per treatment group. *p<0.05 by unpaired two-tailed t-test). (B) Individual tumor growth curves for subcutaneous mT3-2D tumor treated with PBS (n=10), combination BXCL701+anti-PD1 treatment (n=10), combination treatment + NK depletion (n=5), combination treatment + CD8+ T cell depletion (n=5), and combination treatment + NK depletion and CD8+ T cell depletion (n=5). (C) Schematic of rechallenge experiment.